Available online at www.sciencedirect.com

ScienceDirect

Ceramics International 40 (2014) 4499–4505

CERAMICS INTERNATIONAL

www.elsevier.com/locate/ceramint

Synthesis, characterization and magnetic properties of glass ceramics containing nanoparticles of both Ba-hexaferrite and Zn-ferrite

M.A. Azooz, S.A.M. Abdel-Hameed*

Glass Research Department, National Research Center, Dokki, Cairo 12622, Egypt

Received 15 July 2013; received in revised form 21 August 2013; accepted 28 August 2013
Available online 18 September 2013

Abstract

Differential thermal analysis, X-ray diffractometry and transmission electron microscopy were used to study the crystallization behavior of glass ribbons with a composition of 35% BaO, 35% Fe_2O_3, 20% B_2O_3 and 10% TiO_2 (mol.%). Replacement of different amounts of BaO by ZnO was studied. Heat treatment was applied at both 700 and 1000 °C for 1 h with heating rate 3 °C/min. Both Ba-hexaferrite and Zn-ferrite, with crystallite size 2–7 nm, were detected by XRD and TEM. The magnetic properties of ribbons prepared via cooling the melts between steel rollers were measured with a vibrating sample magnetometer. Magnetization saturation (*Ms*) was increased by increasing ZnO, while coercivity (*Hci*) increased by increasing BaO. Partial replacement of Ba by Zn revealed preparation of samples contains both Zn ferrite and Ba hexaferrite which give wide range for engineering application.

Keywords: Ba-ferrite; Zn-ferrite; Glass-ceramics

1. Introduction

Nanoparticles ferro and ferri-magnetic glass-ceramics play an essential role for the future technology, especially in different health care uses, such as cell separation, magnetic resonance imaging contrast agents, hyperthermia treatment of cancer and drug delivery. On the other hand, permanent magnet plays very important role in engineering applications as particulate media for recording high density information [1] as credit, debit, and ATM cards. Speakers and microphones, electric motors and generators are other engineering applications.

The importance of magnetic nanoparticles comes from its remarkable new phenomena, such as super paramagnetism, high field irreversibility, high saturation field, extra anisotropy contributions or shifted loops after field cooling. These phenomena arise from finite size and surface effects that dominate the magnetic behavior of individual.

Barium hexaferrites, owing to their superior properties, have been utilized in various applications as permanent magnets and particulate media for recording high density information. In recent years, the glass crystallization method has been widely used to synthesis various magnetic materials, especially barium hexaferrites. Most investigators have chosen B_2O_3 as a glass former for their base glass compositions. The effects of composition, nucleating agents and heat treatment schedule upon magnetic properties have been reported [2–6]. Borate glass offers many advantages in this process, especially for manufacturing particulate recording media, where the amorphous phase must be leached out and the inherent low chemical durability of borate glasses facilitate the process [1]. However, for other applications, e.g. thin films, where the magnetic phase should be dispersed in a glassy matrix, the glass should be chemically more resistant and not vulnerable to moisture attack.

There have been some attempts to change the properties of matrix glasses by partially replacing B_2O_3 by 10 mol.% SiO_2 in the composition $0.45BaO \cdot 0.25Fe_2O_3 \cdot 0.30B_2O_3$ [4]. It was supposed that in addition to improve the durability of glass, this could decrease the crystallization rate of the melt and

*Corresponding author.
E-mail address: Salwa_NRC@hotmail.com (S.A.M. Abdel-Hameed).

0272-8842/$ - see front matter © 2013 Elsevier Ltd and Techna Group S.r.l. All rights reserved.
http://dx.doi.org/10.1016/j.ceramint.2013.08.124

make it more controllable. However, it was proved that the resultant glass ceramics while showing a relatively high coercivity exhibited a low value of saturation magnetization. In order to increase the values of saturation magnetization, it was attempted to increase the content of Fe_2O_3 to 35 mol.% at the expense of BaO [5]. The above mentioned specimens although exhibited much improved values of *Ms* but generally showed mostly non-uniform and not quite the expected fine microstructures. In order to improve this, it was decided to add TiO_2 as nucleating agents to the main glass composition.

On the other hand, spinel ferrite nanocrystals are regarded as two of the most important inorganic nanomaterials because of their electronic, optical, electrical, magnetic, and catalytic properties. Spinel ferrites have the structure AB_2O_4 in which A and B display tetrahedral and octahedral cation sites, respectively, and O indicates the oxygen anion site. Metal spinel ferrite nanoparticles have the general molecular formula MFe_2O_4 (e.g., M=Zn, Ni, Co, Mn, or Mg), and they have a face-centered cubic (fcc) close packing structure. Among the spinel ferrite compounds, zinc ferrite ($ZnFe_2O_4$) has been studied extensively due to its high electromagnetic performance, excellent chemical stability, mechanical hardness, low coercivity, and moderate saturation magnetization, which make it a good contender for applications as soft magnets and low-loss materials at high frequencies [7].

In this paper, glass ceramic contains both of Ba- and Zn-ferrite nanoparticles was prepared and studied. A comprehensive account of the addition of TiO_2 to these glasses has been given with an emphasis on the microstructural changes and their effect on the magnetic properties.

2. Experimental methods

The chemical compositions of the examined samples are illustrated in Table 1.The samples were signed as Z0, Z0.5 and Z1 according to the percent of ZnO substitute BaO in the batch composition. The batch compositions were mixed well in ball miller for about 15 min.

The calculated batches were melted in platinum 2% Ru crucibles for 2 h after the last traces of the batch constituents had disappeared. The melting was carried out at 1350–1450 °C according to the glass composition using an electric furnace (Vecstar model VF3 UK). The melts were rotated several times 30 min apart to achieve homogeneity. The melts were poured on to a stainless steel plate at room temperature and pressed into a plate 1–2 mm thick by another cold steel plate.

Table 1
Chemical compositions of fifth group in mol.%.

Sample no.	BaO	ZnO	Fe_2O_3	B_2O_3	TiO_2
Z0	35	–	35	20	10
Z0.5	17.5	17.5	35	20	10
Z1	–	35	35	20	10

Thermal behaviors of the prepared samples were examined using differential thermal analysis (DTA). The glass transition temperature (T_g) and the temperature of crystallization (T_c) were evaluated from DTA data. DTA was performed using SETRAM Instrumentation Reulation, Labsys™ TG-DSC16 under inert gas. According to the DTA results the obtained glass were heat treated at different temperatures with heating rate 3 °C/min under reducing atmosphere in a SiC electric furnace to study the effect of heat treatment on the crystallization behavior. It was noticed that the synthesis parameters (such as temperature, time, heating rate, and atmosphere) play a fundamental role for magnetite crystallization.

The identification of the crystalline phases precipitated within the glass-ceramic samples was carried out by X-ray diffraction analysis. Bruker D8 Advanced Instrument adopting Ni-filtered Cu radiation was used in the present investigation. The X-ray diffraction patterns were recorded in a 2θ range of 10–70°.

TEM was used to study microstructure and crystallite size of the prepared samples. The heat treated glasses were crushed and sonically suspended in ethanol and few drops of the suspended solution were placed on an amorphous carbon film held by copper micro grid mesh and then observed under transmission electron microscope.

The magnetic properties of the as prepared and heat treated samples were measured at room temperature using a vibrating sample magnetometer (VSM; 9600-1 LDJ, USA) in a maximum applied field of 20 kOe. From the obtained hysteresis loops, the saturation magnetization (*Ms*), remanence magnetization (*Mr*) and coercivity (*Hci*) were determined.

3. Results and discussion

Fig. 1 reveals DTA traces of samples under investigation. Z0 sample (with zero ZnO) revealed endothermic effect at 548 °C and two exothermic effects at 674 and 725 °C, respectively. Appearance of two exothermic peaks means crystallization of two different phases or crystallization of a phase followed by transformation of this phase to another structure form; this will be confirmed by XRD later. DTA of Z0.5 and Z1 revealed one exothermic peak corresponding to crystallization of one crystallized phase followed by sharp endothermic effect which may be due to partial remelting of the crystallized phase.

Heat treatment of these samples at 700 and 1000 °C for 1 h with heating rate 3 °C/min under reducing atmosphere was done.

Figs. 2–4(a)–(c) reveal XRD analysis of Z0, Z0.5 and Z1 after quenching from melting temperature, heat treatment at 700 °C/1 h and 1000 °C/1 h, respectively, with heating rate 3 °C/min under reducing atmosphere.

From Fig. 2, for Z0 sample, it is noticed that, in general the major of detectable peaks can be indexed as belonging to the barium hexaferrite phase ($BaFe_{12}O_{19}$), in the standard data (card no. 27-1029) immersed in amorphous glassy phase. Traces of hematite were observed in quenched sample, while

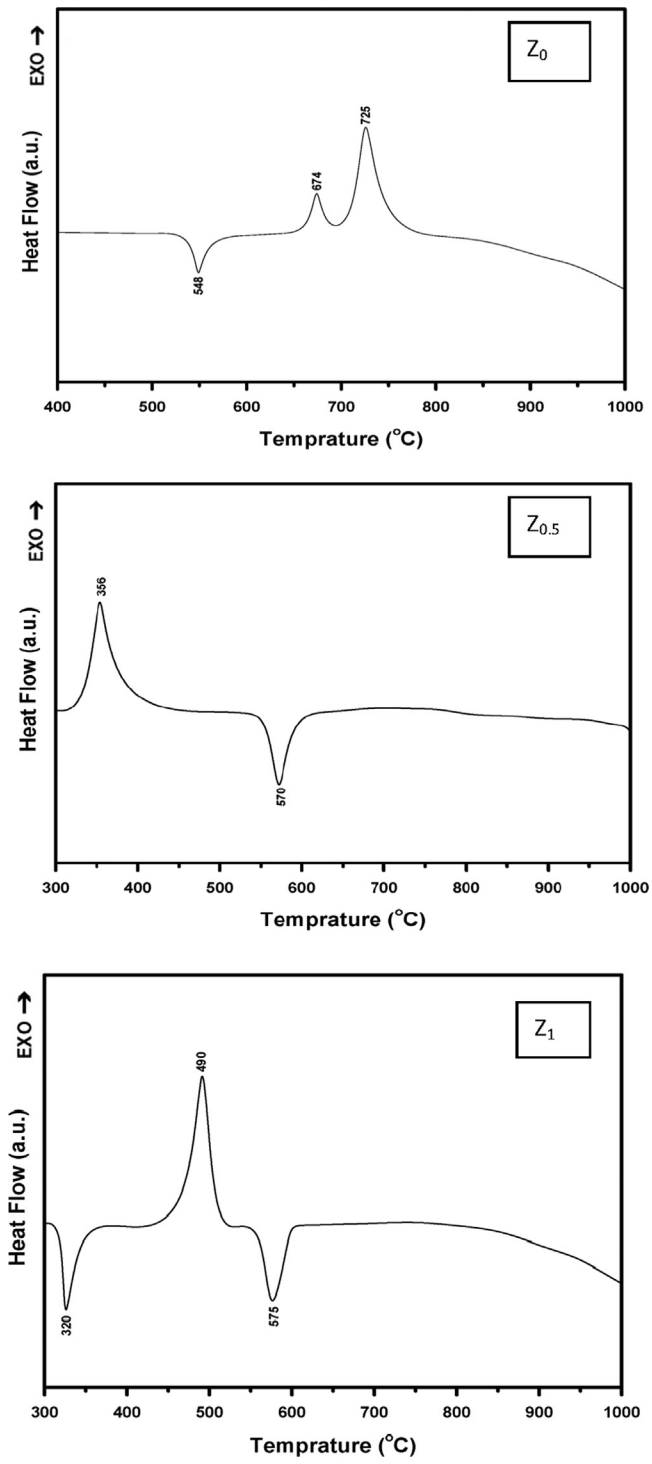

Fig. 1. DTA traces of Z0, Z0.5 and Z1 after cooling from melting temperatures.

traces of $Fe_2Ti_3O_9$ phase (card no. 29-1494) were detected after heat treatment at both 700 °C and 1000 °C.

XRD of Z0.5 (Fig. 3) revealed crystallization of Zn-ferrite beside traces of hematite immersed in amorphous glassy phase after quenching from melting temperature. The amount of hematite was increased by applying heat treatment at 700 °C/1 h due to the partial oxidation of the iron. Partial remelting of the above mentioned phases was done after applying heat

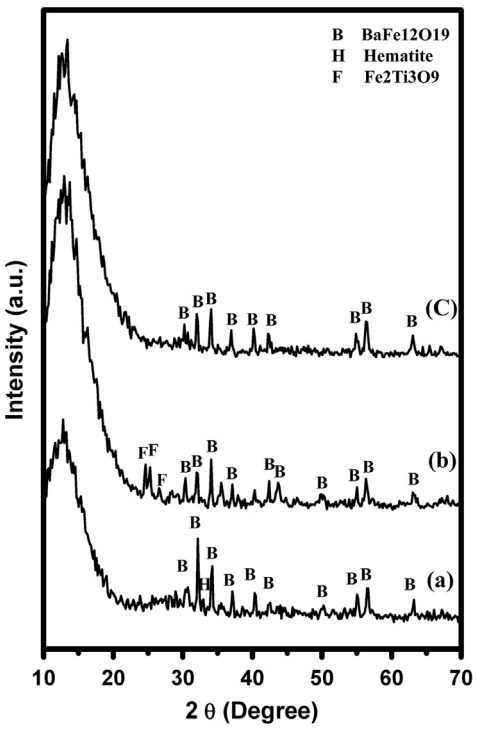

Fig. 2. XRD analysis of Z0 sample (a) as quenched sample, (b) after heat treatment at 700 °C/1 h and (c) after heat treatment at 100 °C for 1 h.

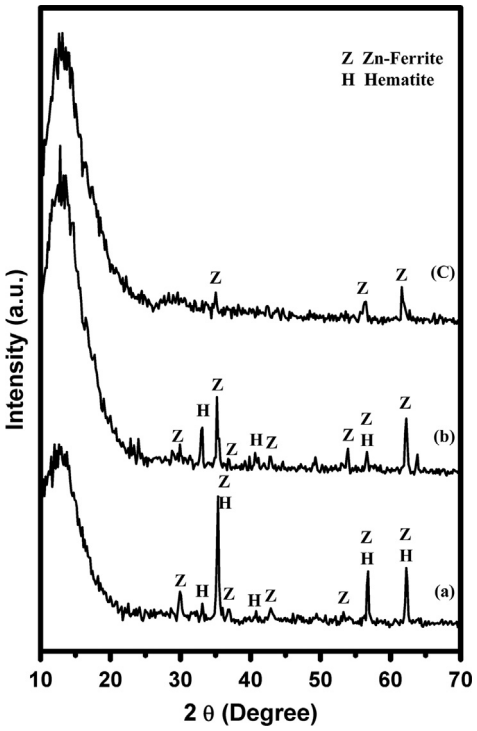

Fig. 3. XRD analysis of Z0.5 sample (a) as quenched sample, (b) after heat treatment at 700 °C/1 h and (c) after heat treatment at 1000 °C for 1 h.

treatment at 1000 °C/1 h which is revealed by significant decrease in the peaks intensity and increasing in the hump corresponding to amorphous glassy phase in the region 4–25 °Θ.

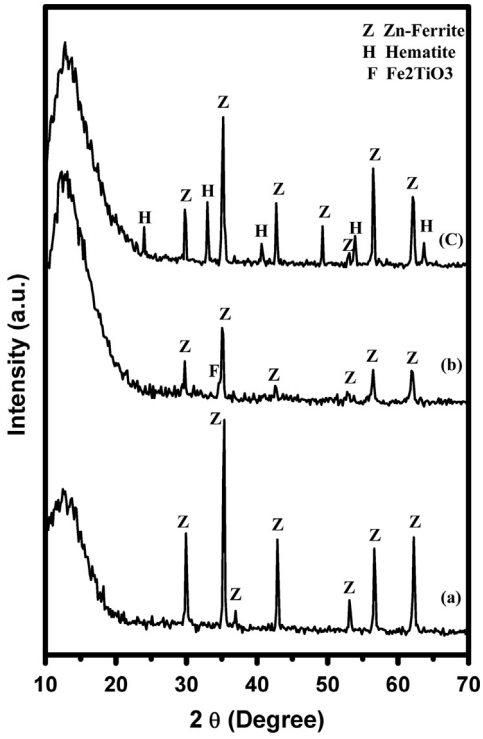

Fig. 4. XRD analysis of Z1 sample (a) as quenched sample, (b) after heat treatment at 700 °C/1 h and (c) after heat treatment at 1000 °C for 1 h.

XRD for Z1 (Fig. 4) revealed crystallization of large amount of pure Zn-ferrite which is mirrored by high peaks intensity after quenching from melting temperature. Minor amounts of Fe_2TiO_4 phase (card no. 24-0537) were detected after applying heat treatment at 700 °C/1 h. Heat treatment at 1000 °C/1 h revealed crystallization of Zn-ferrite as the major crystalline phase with minor hematite and β-Fe_2O_3. It is noted that applying heat treatment to the samples allows more movement and mobility to the ions revealing different crystalline phases.

Transmission electron microscopy (TEM) was performed in order to investigate the possibility of micro-twinning and the homogeneity of the materials. TEM can determine exactly the size of each individual crystal, on the other hands. Particle size measurements can be viewed from TEM measurements, in a sense of approximation.

TEM of quenched samples are shown in Figs. 5–7. In general nanoparticle sized was crystallized in all samples. Z0 sample clearly shows the formation of branched chains formed from regular spheres of Ba-hexaherrite almost the same size ranged from 2 to 7 nm (Fig. 5). TEM of Z0.5 sample (Fig. 6) revealed dispersive coagulation of rounded crystals in the crystallite size 5–7 nm from Zn-ferrite phase. The same behavior was observed by Z1 sample (Fig. 7) which revealed dispersive coagulation of about 50–70 nm, each coagulation contains particles of Zn-ferrite in the range of 10–40 nm.

Increasing the crystallite size with increasing Zn ions can be attributed to the presence of Zn after Ba in the periodic table which makes it have lower ionic volume and higher electro-negativity; these two properties facilitate its mobility and consequently leading to easier in crystallization process and crystallite size.

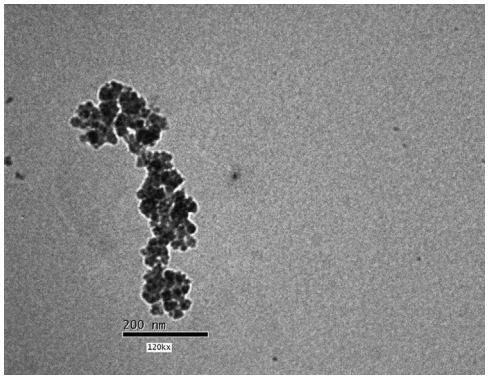

Fig. 5. TEM of Z0 after quenching fro melting temperature.

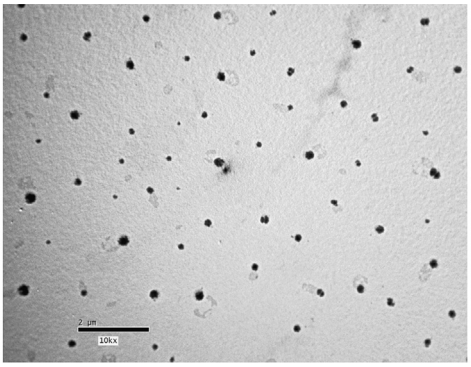

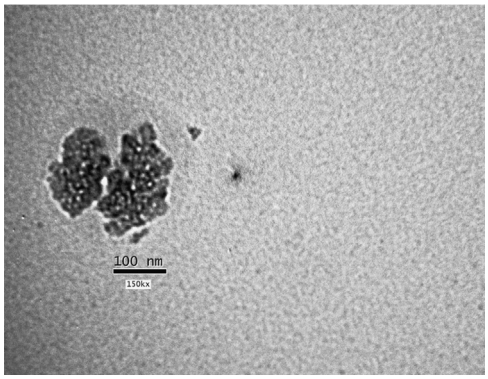

Fig. 6. TEM of Z0.5 after quenching fro melting temperature.

3.1. Magnetic properties

Fig. 8 depicts the room temperature magnetic hysteresis (M-H) loops of Z0, Z0.5 and Z1 after quenching from melting temperature at magnetic field strength of ± 20 kOe. Table 2 displays the relevant magnetic parameters; saturation magnetization (*Ms*), coercivity (*Hci*), remanence (*Mr*) and area obtained from M-H loops. *Ms* increases with increase in ZnO concentration and shows a trend to saturate for Z1 with the maximum value of about 24.36 emu/g. The increase in

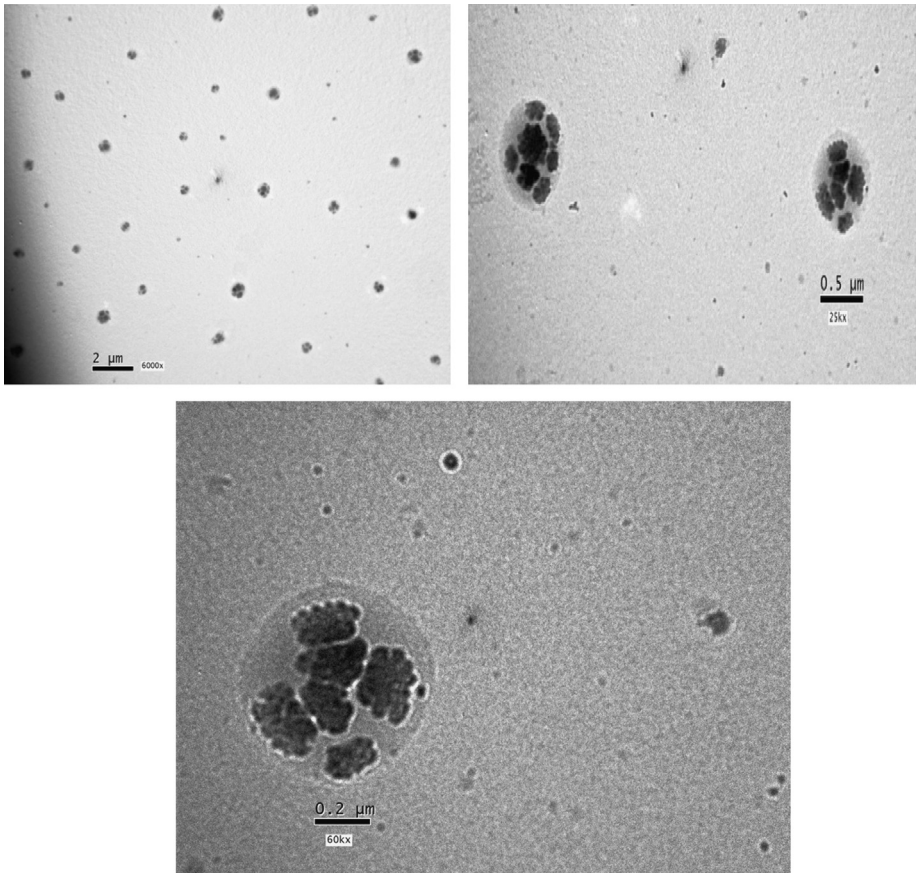

Fig. 7. TEM of Z1 after quenching fro melting temperature.

saturation magnetization with increase in ZnO concentration could be attributed to the development of $ZnFe_2O_4$ phase in the samples, as observed in Figs. 3 and 4.

These changes can be correlated with the changes obtained in the values of crystallite sizes. The dependence of the magnetization and magnetic moment on the grain size can be explained on the basis of changes in the exchange interaction between tetrahedral and octahedral sub-lattices. In addition, the influence of cationic stoichiometry, the preferential occupancy in the specific sites, magneto crystalline anisotropy, canting effect and dipolar interactions between the projected moment on the surface of nanoparticles should be considered and hence the observed magnetic property is accumulative effect of these interactions [9,10].

Zn^{2+}(3d10) is a non-magnetic ion and has a strong tendency for occupying tetrahedral sites and thus the B–B sublattice interaction becomes stronger. When Zn^{2+} content increased, according to the estimated cation distribution, it prefers to occupy the octahedral sites which will results in weakening the A–B exchange and decreasing the magnetization. The increase in the magnetization value at Z1 indicates the preferential occupation of zinc ions by tetrahedral sites with strength the B–B interaction and increasing magnetization. Several investigators [11–13] suggested the preferential occupancy of Zn^{2+} ions by octahedral sites depending on the utilized preparation method and nano-sized characteristics. From all the above we can conclude that all the investigated ferrites samples show reasonably good magnetic properties at room temperature and the high Zn^{2+} substitution can enhance *Ms*. On the other hand, the variation of the coercivity values with Zn-substitution can be explained on the basis of the magneto-crystalline anisotropy [14].

Magnetic anisotropy, shape and dimension of the crystals, residual stress and crystal imperfections influence the coercivity and remanence magnetization [8]. The coercivity of the samples decreases with increase in ZnO concentration in the quenched samples. The coercive field slowly decreases with increase in average crystallite size of $ZnFe_2O_4$ as shown in Table 2.

Zn-ferrite has a magnetite-like structure in which some of the iron ions in the tetrahedral site of the magnetite crystal are substituted by zinc ions [5]. In the case of Fe_3O_4 nanocrystals, the degree of ordering of the magnetic moment in the individual crystallites increases with increase in crystallite size until a well ordered single domain structure is reached at 40 nm. Further increase in crystallite size increases the number of magnetic domains in the individual crystallites, thereby leading to a decrease in coercivity [15].

Area of the hysteresis loop increases with increase in Zn-ferrite content. The largest area is obtained for the Z1, which

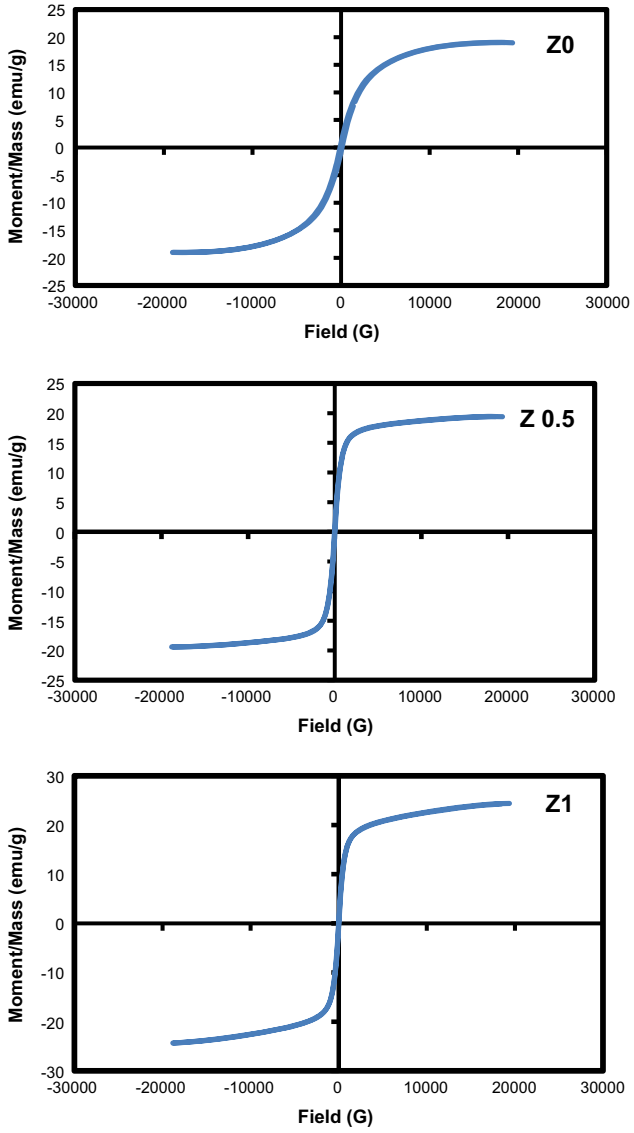

Fig. 8. Effect of ZnO additions on the hysteresis loop of quenched samples.

Table 2
Magnetic parameters for quenched samples.

Sample no.	*Ms* (emu/g)	*Hci* (G)	*Mr* (emu/g)
Z0	19.05	112.21	0.88
Z0.5	19.43	23.95	0.58
Z1	24.36	16.08	0.51

also exhibits the highest saturation magnetization and lowest coercivity among the samples studied. Since the area under the hysteresis loop is proportional to the energy loss and hence the heat generated by a sample under an alternating field, samples with higher amount of Zn-ferrite phase are capable of generating more heat. The large variation in the area under the loops for these samples provides a means for controlled heat generation by appropriate choice of sample.

The remanence signifies the ability of a magnetic material to be spontaneously magnetized, even in the absence of external magnetic field. It is noticed that, an excessive addition of ZnO slightly degrades the remanent magnetization *Mr*. The value of *Mr* was increased as the amount of impurities increased; therefore, the increase in *Mr* resulted from the presence of hematite traces in both of Z0 and Z0.5 while decrease of *Mr* in Z1 was attributed the presence of pure zinc iron oxide in quenched samples.

It is noticed that, μr (relative permeability) is » 1 consequently this materials are considered as ferromagnetic material.

4. Conclusions

Synthesis, characterization and magnetic properties of glass ceramics containing nanoparticles of both Ba-hexaferrite and Zn-ferrite were studied. Partial replacement of Ba ions by Zn ions in the system was studied. Barium hexaferrite phase is the major crystalline phase crystallized in sample free from Zn. Increasing Zn ions revealed increasing the in saturation magnetization and crystallite size. TEM revealed crystallization of nanocrystallite size < 40 nm. Partial replacement of Ba by Zn revealed preparation of samples contains both Zn ferrite and Ba hexaferrite which give wide range for engineering application.

Acknowledgments

This project was supported financially by the Science and Technology Development fund (STDF), Egypt, Grant No 1044.

References

[1] M. Mirkazemi, V.K. Marghussian, A. Beitollahi, S.X. Dou, D. Wexler, K. Konstantinov, Effect of ZrO_2 nucleant on crystallisation behaviour, microstructure and magnetic properties of BaO–Fe_2O_3–B_2O_3–SiO_2 glass ceramics, Ceramics International 33 (2007) 463–469.
[2] K. Watananabe, K. Hoshi, Crystallisation kinetics of fine barium hexaferrite, $BaFe_{12}O_{19}$ particles in a glass matrix, Physics and Chemistry of Glasses 40 (1999) 75–78.
[3] L. Rezlescu, E. Rezlescu, P.D. Popa, N. Rezlescu, Fine barium hexaferrite powder prepared by the crystallisation of glass, Journal of Magnetism and Magnetic Materials 193 (1999) 288–290.
[4] V.K. Marghussian, A. Beitollahi, M. Haghi, The effect of SiO_2 and Cr_2O_3 additions on the crystallisation behaviour and magnetic properties of a B_2O_3–BaO–Fe_2O_3 glass, Ceramics International 29 (2003) 455–462.
[5] M. Mirkazemi, V.K. Marghussian, A. Beitollahi, Microstructure and magnetic properties of BaO–Fe_2O_3–B_2O_3–SiO_2 glass ceramics, Ceramics International 32 (2006) 43–51.
[6] M. Mirkazemi, A. Beitollahi, V.K. Marghussian, Microstructure and magnetic properties of BaO–Fe_2O_3–B_2O_3–SiO_2 glass ceramics with ZrO_2 as nucleating agent, Physica Status Solidi (C) 1 (12) (2004) 3216–3226.
[7] Mahmoud Goodarz Naseri, Elias B. Saion, Mansor Hashima, Abdul Halim Shaari, Hossein Abasstabar Ahangard, Synthesis and characterization of zinc ferrite nanoparticles by a thermal treatment method, Solid State Communications 151 (2011) 1031–1035.
[8] A. Saqlain, M.U. Shah, S.H. Alam, Effect of aligning magnetic field on the magnetic and calorimetric properties of ferrimagnetic bioactive glass ceramics for the hyperthermia treatment of cancer, Materials Science and Engineering 31 (2011) 1010–1016.
[9] R.H. Kodama, A.E Berkowitz, Physical Review B 59 (1999) 6321.
[10] A. Alarifi, N.M Deraz, S Shaban, Journal of Alloys and Compounds 486 (2009) 501.
[11] H. Kavas, A. Baykal, M.S. Toprak, Y. Kseoglua, M. Sertkol, B. Aktas, Journal of Alloys and Compounds 479 (2009) 49.

[12] C. Yao, Q. Zeng, G.F. Goya, T. Torres, J. Liu, H. Wu, M. Ge, Y. Zeng, Y. Wang, J.Z. Jiang, Journal of Physical Chemistry C 111 (2007) 12274.
[13] S. Bid, S.K. Pradhan, Materials Chemistry and Physics 82 (2003).
[14] M.A. Gabal, R.S. Al-Luhaibi, Y.M. AlAngari, Effect of Zn-substitution on the structural and magnetic properties of Mn–Zn ferrites synthesized from spent Zn–C batteries, Journal of Magnetism and Magnetic Materials, 348 (2013) 107–112.
[15] Salwa A.M. Abdel-Hameed, Rawhia L. Elwan, Effect of La_2O_3, CoO, Cr_2O_3 and MoO_3 nucleating agents on crystallization behavior and magnetic properties of ferromagnetic glass–ceramic in the system $Fe_2O_3 \cdot CaO \cdot ZnO \cdot SiO_2$, Materials Research Bulletin 47 (5) (2012) 1233–1238.